Internal optimization of the texture component approximation method

Internal optimization of the texture component approximation method

D. Nikolayev[1], T. Lychagina[1], M. Rusetsky[2], A. Ulyanenkov[3] and A. Sasaki[4]
[1] Frank Laboratory of Neutron Physics, Joint Institute for Nuclear Research, Dubna, Russia
[2] Belarusian State University, Minsk, Belarus
[3] Rigaku Europe SE, Ettlingen, Germany
[4] Rigaku Corporation, Tokyo, Japan
E-mail: dmitry@nf.jinr.ru

Abstract. The component approximation method for the reconstruction of orientation distribution function (ODF) is based on the assumption that the texture could be presented as a weighted linear combination of distributions depending on the parameters, which are related to the position of bell shaped function in orientation space and to the dispersion. The method uses a minimization procedure to obtain the values of ODF parameters. Traditionally, the mean-square deviation of the measured and recalculated pole figures is minimized. However, the quantitative measure of the fit is RP value which differs from the mean-square deviation. In the present work it is suggested to minimize the RP value to obtain ODF parameters. We are using Trust Region method for solving a non-linear optimization problem. The convergences of the proposed method for different minimized functional are compared. We also illustrate a usage of the different objective function on modeling data for the cubic crystalline symmetry. This study is fulfilled using new RIGAKU software for quantitative texture analysis.

1. Introduction

The core problem of the quantitative texture analysis is the ODF reconstruction from the measured pole figures. The component approximation method [1-3] is recently developed for the ODF reconstruction. One of the advantages of the method is a clear physical meaning of the computed parameters. The central difficulty of this method is the nonlinear minimization problem which should be solved for the parameters in question.

2. Component approximation method

Before introduction of the ODF [4] the texture had been characterized by the analysis of pole figures, which assigned one or several preferred orientations explaining the bell shaped peaks on the measured pole figures. The general idea of the component approximation method is a formalization and quantification of such approach. The texture is assumed to be caused by a linear combination of the components centered at the positions of the preferred orientations in the orientation space or rotation group SO(3). Formally this means the ODF can be presented as follows:

$$f(g) = FON + \sum_{n=1}^{NUMB} A_n f^{p}(g, g_{0n}, \varepsilon_n) + \sum_{k=1}^{NUMF} A_k f^{f}(g, \bar{n}_t, g_o \bar{n}_t, \varepsilon_k) \qquad (1)$$

Here $f^{p}(g, g_{0n}, \varepsilon_n)$ and $f^{f}(g, \bar{n}_t, g_o \bar{n}_t, \varepsilon_k)$ are the peak and the fiber component, respectively. Components are non-negative functions integrating to 1 on SO3 (to be probability density) The values A_n and A_k are the weights, ε_n and ε_k are the parameters describing the width of the components, and $g_{0n} = (\alpha_n, \beta_n, \gamma_n)$ are parameters describing the peak position or position of the ideal orientation on the SO(3) group, $NUMB$ is the number of peak components. $\bar{n}_t = (\theta_y, \varphi_y)$, $g_o \bar{n}_t = (\theta_h, \varphi_h)$ are the parameters describing the fiber component position, $NUMF$ is the number of fiber components, and FON is the background value or isotropic component weight. Weights are non-negative and sum up to 1

$\left(FON + \sum_{n=1}^{NUMB} A_n + \sum_{k=1}^{NUMF} A_k = 1 \right)$. It is important to note that this is a constrained to the optimization problem.

The recalculated pole figures for the ODF in the form (1) are expressed in the following way:

$$P^r{}_{\vec{h}_i}(\vec{y}) = FON + \sum_{n=1}^{NUMB} A_n P_{\vec{h}_i}{}^p(\vec{y}_j, g_{0n}, \varepsilon_n) + \sum_{k=1}^{NUMF} A_k P_{\vec{h}_i}{}^f(\vec{y}_j, \vec{n}_t, g_o\vec{n}_t, \varepsilon_k) \qquad (2)$$

For a special appearance of the components, the expression for the recalculated pole figures could also be presented in the forms given below:

• Brownian motion distribution

$$P_{\vec{h}}^p(\vec{y}) = \sum_{l=0}^{\infty}(2l+1)\exp(-l(l+1)\varepsilon^2)P_l(\cos\theta_0) \qquad \cos\theta_0 = \left(\vec{y}, g_0^{-1}\vec{h}\right) \qquad (3)$$

$$P_{\vec{h}}^f(\vec{y}, \vec{n}_t) = \sum_{l=0}^{\infty}(2l+1)\exp(-l(l+1)\varepsilon^2)P_l(\cos\theta_1)P_l(\cos\theta_2) \quad \cos\theta_1 = \left(\vec{h}, g_0^{-1}\vec{n}_t\right) \quad \cos\theta_2 = \left(\vec{y}, \vec{n}_t\right)$$

$$f^p(g, g_0, \varepsilon) = \sum_{l=0}^{\infty}(2l+1)\exp(-l(l+1)\varepsilon^2)\frac{\sin(l+\frac{1}{2})t}{\sin\frac{t}{2}} \quad \cos t = [Tr(gg_0{}^{-1})-1]/2$$

$$f^f(g, g_0, \varepsilon, n_t) = \sum_{l=0}^{\infty}(2l+1)\exp(-l(l+1)\varepsilon)P_l(\cos\tau) \quad \cos\tau = (g\vec{n}_t, g_o\vec{n}_t)$$

• Fisher distribution

$$P_{\vec{h}}^p(\vec{y}) = \frac{1}{I_0(S)-I_1(S)}I_0\left(S(1+\cos\theta_0)/2\right)\exp(S(\cos\theta_0-1)/2) \qquad \cos\theta_0 = \left(\vec{y}, g_0^{-1}\vec{h}\right) \qquad (4)$$

$$P_{\vec{h}}^f(\vec{y}, \vec{n}_t) = \frac{1}{I_0(S)-I_1(S)}I_0\left(S\sin\theta_1\sin\theta_2\right)\exp(S\cos\theta_1\cos\theta_2)$$

$$f^p(g, g_0, S) = \frac{1}{I_0(S)-I_1(S)}\exp(S\cos t) \quad \cos t = [Tr(gg_0{}^{-1})-1]/2$$

$$f^f(g, g_0, S, \vec{n}_t) = \frac{S}{\sinh S}\exp(S\vec{h}\cdot g\vec{n}_t)$$

These both distributions have a similar nature as normal distribution. There are two more distributions, namely Lorentz [5] and the hyperspherical de la Vallée Poussin kernel [6], which also can be used as texture components. Finally, the following distribution approximates [7] the normal one, too:

$$P_{\vec{h}}^p(\vec{y}) = \frac{\sigma}{\cos\theta_0}\left(\frac{1}{\cos^2\theta_0}+\frac{1}{2\sigma}\right)\exp\left(-\sigma\tan^2(\theta_0/2)\right) \qquad \cos\theta_0 = \left(\vec{y}, g_0^{-1}\vec{h}\right) \qquad (5)$$

$$f^p(g, g_0, \sigma) = \frac{\sigma\sqrt{\pi\sigma}}{\cos^4(t/2)}\exp(-\sigma\tan^2(t/2))$$

The distributions with a normal nature do not allow the isotropic generalization, and only the last one has a simple form, which does not contain the series or integrals. The main problem of the quantitative texture analysis thus can be formulated and resolved as follows. For the existing NPF measured pole figures, we can imply the texture is described by *NUMF* fiber components and *NUMB* peak components. The certain suggestions can be made about the

initial values of the components parameters using the pole figure pictures. By using the form (2) of the recalculated pole figures, the component method is applied to find the corresponding parameters of peak and fiber components, which are found from the minimum of the functional:

$$\Phi(P_{\bar{h}_i}^{\exp}(\bar{y}_j), P^r{}_{\bar{h}_i}(\bar{y})) \to min\,.$$

The total number of the parameters to minimize is $5 \cdot NUMB + 6 \cdot NUMF + NPF + 1$. There are several approaches for the choice of the functional. The old approach is based on the least squares minimization with the functional:

$$\sqrt{\sum_{i=1}^{NPF}\left(P_{\bar{h}_{i(}}^{\exp}(\bar{y}_j) - N_i \times \left(\sum_{n=1}^{NUMB} A_n P_{\bar{h}_i}(\bar{y}_j, g_{0n}, \varepsilon_n) + \sum_{k=1}^{NUMF} A_k P_{\bar{h}_i}(\bar{y}_j, \bar{n}_t, g_o \bar{n}_t, \varepsilon_k) \right) - FON \right)^2} \to min \qquad (6)$$

In [8-10] a set of alternative functionals had been proposed. We consider in this work the new approach with the functional in the form of RP value. The RP values are defined as follows [5]:

$$RP_i = \sum_{j=1}^{J} 100\% * \frac{\left| P_{\bar{h}_i}(\bar{y}_j) - P_{\bar{h}_i}^M(\bar{y}_j) \right|}{P_{\bar{h}_i}(\bar{y}_j)} \Theta\left(\zeta, P_{\bar{h}_i}(\bar{y}_j)\right) \Big/ \sum_{j=1}^{J} \Theta\left(\zeta, P_{\bar{h}_i}(\bar{y}_j)\right), \quad \Theta(\zeta, x) = \begin{cases} 0, & x < \zeta \\ 1, & x \geq \zeta \end{cases} \qquad (7)$$

Here ζ is a sensitivity level, and the minimization is fulfilled by the TRUST REGION method [11], which has been recently developed for finding of global maxima in the nonlinear optimization problems.

3. Numerical examples

The solution of the nonlinear optimization problem requires an essential number of the recalculated pole figures, computed with different parameters. To reach a reliable result in a reasonable time, the component function must be computed as fast as possible. Despite the distributions (3) and (4) have very useful features (entropy maximization, fundamental solution of the diffusion equation, etc.), the distribution (5) is much easier and faster for computation. The figure 1 shows the correspondence between all these distributions.

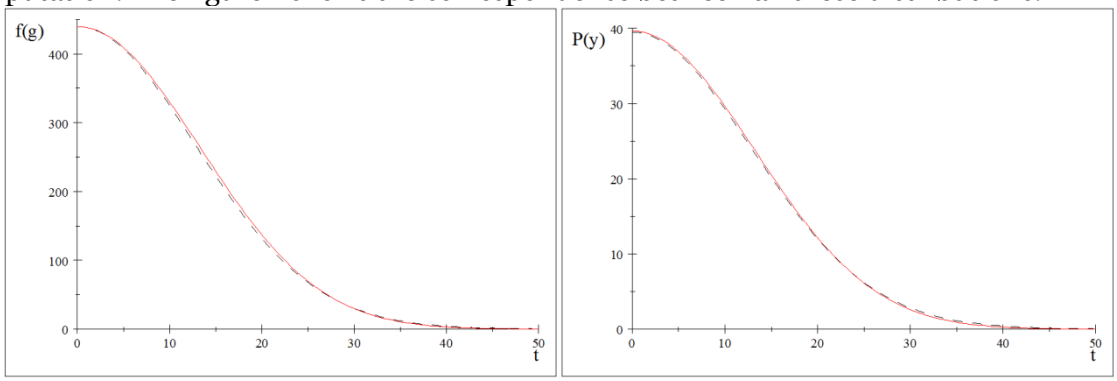

Fig 1. The illustration of the distributions used in calculations. The parameters of the distributions are S = 20, σ = 39.483, ε^2 =2.5435×10^{-2}. All the parameters correspond to a full width at the half maximum b = 30.17°. The dashed line is for distribution (3) and (4), the solid line is for (5).

For a smaller value of width, these distributions become indistinguishable, and thus the distribution with a fastest computation time can be used, which is the distribution (5). Because of all these tree distributions approximate each other quite well, we can use any of them for the further analysis after a proper adjustment of parameters. For example, the simplest form of C coefficients has the distribution (3), and we used formula (3) for the peak

components and (4) for the fiber components to generate numerical example. The connection between the parameters describing the width of the components ε and b is presented in [12-13].

Table 1. Summary of the numerical experiment

Parameter	model	initial assumption	optimized (old approach)	optimized (new approach)
$g_0(\alpha,\beta,\gamma)$	$\{45^\circ,45^\circ,45^\circ\}$	$\{46^\circ,46^\circ,46^\circ\}$	$\{45.01^\circ,45.04^\circ,44.96^\circ\}$	$\{45.16^\circ,45.20^\circ,45.16^\circ\}$
b_{peak}	15°	15°	14.97°	14.92°
A_{peak}	0.450	0.450	0.447	0.449
$\vec{n}_t(\theta_y,\varphi_y)$	$\{10^\circ,10^\circ\}$	$\{11^\circ,11^\circ\}$	$\{10.34^\circ,11.00^\circ\}$	$\{10.30^\circ,10.99^\circ\}$
$g_0\vec{n}_t(\theta_h,\varphi_h)$	$\{10^\circ,10^\circ\}$	$\{11^\circ,11^\circ\}$	$\{10.18^\circ,10.18^\circ\}$	$\{10.21^\circ,10.21^\circ\}$
b_{fiber}	15°	15.66°	15.67°	15.67°
A_{fiber}	0.450	0.450	0.454	0.453
FON	0.10	0.10	0.096	0.101

The corresponding pole figures are shown in the figure 2. The functionals (6) and (7) have been used for nonlinear minimization procedure, and the distribution (5) is applied during the fitting procedure. The results of the fit are collected in the table 1.

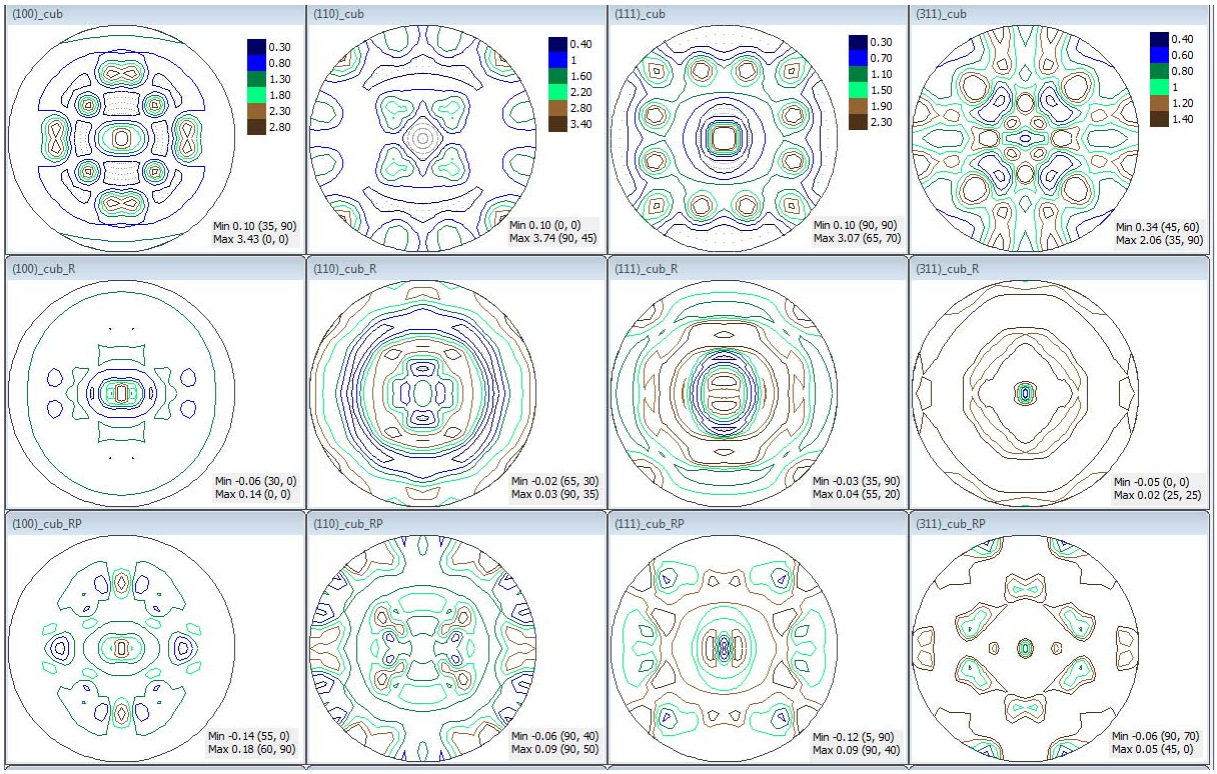

Fig 2. The model pole figures (100), (110), (111) and (311) for cubic crystal and orthorhombic sample symmetry simulated for one peak and one fiber component with parameters presented in the table 1 (1st row). The spatial distribution of the recalculation error (2nd-3rd rows for the old and new approaches respectively).

Both procedures converge to the similar correct results. The minimization procedure with functional (7) converges with 33 iterations and mean RP=1.93, whereas ones with functional (6) converges with 18 iterations and mean RP=1.05. The recalculated pole figures are indistinguishable with the modeled ones. The functional (6) evidently converges faster due to a less number of iterations required, and the RP mean value over all pole figures is slightly smaller.

4. Discussion

The component approximation method has a number of evident advantages, which are demonstrated in the paper. The reconstructed parameters have a clear physical meaning. The number of pole figures required for reconstruction of ODF is relatively small. However, the component approximation method has some disadvantages. The method is not automatic, i.e. the researcher needs to choose the number and the type (peak or fiber) of components. In the case of not distinguishable peak and fiber types of components, the method is not recommended for use to avoid a misinterpretation of the texture character. The method is sensitive to a self-consistency of the measured pole figures. The measured pole figures must be self-consistent, but due to experimental errors this condition can be violated. Another challenging factor influencing the application of the method is a use of non-linear minimization problem. The results of the ODF reconstruction by component approximation method depend on the specific component choice and the functional to be minimized, which both are the key levers to optimize the analysis. The RP value is found to be more stable but less sensitive parameter for minimization procedure and the functional (6) seems to be more sensitive one. As a consequence, for example, for the noisy data the using of the RP value is preferable.

Acknowledgment

The present work has been initiated and supported by Rigaku Corporation.

References

[1] Nikolayev D I, Savyolova T I and Feldman K 1992 *Textures and Microstructures* **19** 9
[2] Bucharova T I and Savyolova T I 1993 *Textures and Microstructures* **21** 161
[3] Bermig G, Tobisch J, Richter K and Helming K 1993 *Material Science Forum* **133-136** 163
[4] Wassermann G and Greven J 1962 *Texturen metallischer Werkstoffe* (Berlin: Springer Verlag)
[5] Matthies S, Vinel G W and Helming K 1987 *Standard Distributions in Texture Analysis* (Berlin: Akademieverlag)
[6] Schaeben H 1997 *Phisica Status Solidi (b)* **200** 367
[7] Ivanova T M and Nikolayev D I 2001. *Physica Status Solidi (b)* **228** 3 825
[8] Barton N R, Boyce D E, Dawson P R, 2002 *Textures and Microstructures*, **35(2)** 113
[9] Bernier J V, Miller M P and Boyce D E 2006 *J. Appl. Cryst.* **39** 69
[10] Hielscher R and Schaeben H 2008 *J. Appl. Cryst.* **41** 1024
[11] Conn A R, Gould N I and Toint P L 2000 Trust-region Methods. SIAM Society for Industrial & Applied Mathematics, Englewood Cliffs, New Jersey, MPS-SIAM Series on Optimization edition.
[12] Lychagina T A, Nikolayev D I and Wagner F 2009 *Texture, Stress and Microstructure*, 237485
[13] Lychagina T A and Nikolayev D I 2003 *Physica Status Solidi (a)*, **195(2)** 322